X-ray microprobe of optical strong-field processes

L. Young[a,*], R.W. Dunford[a], C. Hoehr[a], E.P. Kanter[a], B. Krässig[a],
E.R. Peterson[a], S.H. Southworth[a], D.L. Ederer[a,1], J. Rudati[b], D.A. Arms[b],
E.M. Dufresne[b], E.C. Landahl[b]

[a]*Chemistry Division, Argonne National Laboratory, Argonne, IL 60439, USA*
[b]*Advanced Photon Source, Argonne National Laboratory, Argonne, IL 60439, USA*

Accepted 8 December 2005

Abstract

A time-resolved X-ray microprobe to study optical strong-field processes has been developed. Individual atoms or molecules located within the strong-field environment created by a focused ultrafast laser are probed by undulator-produced X-ray pulses to achieve spatial, temporal, spectral and polarization selectivity. Approximately 10^6 monochromatic X-rays per 100-ps pulse are focused into a $\sim 10 \, \mu m$ spot to selectively probe atoms in focal volumes where intensities up to $10^{15} \, W/cm^2$ can be present. In this paper, we describe the time-resolved X-ray microprobe and provide some illustrative examples from our work studying strong-field phenomena such as laser-modified absorption spectra, Coulomb explosion, transient laser-produced plasmas and molecular alignment.
© 2006 Elsevier Ltd. All rights reserved.

1. Introduction

The study of structural dynamics on an ultrafast time scale is a prime motivation for the construction of large-scale next-generation X-ray sources, i.e. free electron lasers (XFELs), such as the Linac Coherent Light Source (Arthur et al., 2002) and the Tesla Test Facility (Tschentscher, 2004). These new sources will access the sub-picosecond timescale with very high single pulse fluence ($\sim 10^{13}$ X-rays/200 fs pulse) in comparison with current synchrotron sources ($\sim 10^8$ X-rays/100 ps pulse) and laser-produced plasma sources ($\sim 4 \times 10^6$ X-rays/

sr/100 fs pulse) (Bargheer et al., 2004). X-rays are particularly valuable in ultrafast dynamics research, since they provide complementary information to that available from optical and charged particle probes. X-rays yield direct information on atomic positions and chemical bond lengths, unlike ultrafast optical probes (Zewail, 2003). X-rays penetrate to probe isolated molecules in solution, buried interfaces and bulk material response, unlike recently developed ultrafast electron sources (Zewail, 2005; King et al., 2005; Siwick et al., 2003). In addition, tunable X-rays from synchrotron sources provide chemical, elemental and polarization specificity (Stöhr, 1996). To this suite of synchrotron basics, one can add "ultrafast" temporal *and* "ultrasmall" spatial information using the laser-pump/X-ray microprobe method described here, thus enabling new studies of the response of atoms and molecules to strong-optical fields.

*Corresponding author. Tel.: +1 630 252 8878;
fax: +1 630 252 6210.
E-mail address: young@anl.gov (L. Young).
[1]Permanent address: Tulane University, New Orleans, LA 70118, USA.

Recently, there has been an explosion of activity at third-generation light sources using pump-probe techniques to track structural dynamics with ~100 ps X-ray pulses. These studies have been of solid-state materials (~10^{22} atoms/cm^3) and solvated species (~10^{19} molecules/cm^3). In ordered solid-state materials, phase-transitions and phonon propagation have been studied extensively, primarily using X-ray diffraction techniques (Sondhauss et al., 2005; DeCamp et al., 2003; Reis et al., 2001; Lindenberg et al., 2000). In some of these studies, the time resolution was extended below the X-ray pulse duration to the few ps level through the use of X-ray streak cameras. Particularly noteworthy is the recent demonstration using ~100 femtosecond pulses from a laser-slicing source (Schoenlein et al., 2000) to study metal–insulator phase-transition dynamics with extended X-ray absorption techniques (Cavalleri et al., 2005). Studies of photoinduced structural dynamics of solute molecules have been done using both X-ray absorption spectroscopy (Chen et al., 2001; Saes et al., 2003) and X-ray diffraction (Neutze et al., 2001; Plech et al., 2004). Some recent achievements include the time-resolved study of chemical reactions and the isolation of a molecular transition state in solution by X-ray diffraction (Davidsson et al., 2005; Ihee et al., 2005). Access to the subpicosecond regime with hard X-rays has already started with experiments on crystal melting at the Sub-Picosecond Pulse Source (SPPS), the precursor to the LCLS (Lindenberg et al., 2005).

Our experiments, in contrast, focus on gas phase samples ($\leqslant 10^{14}$ cm^3) with no long-range order. Also in contrast to other pump-probe studies, we use strongly focused X-ray beams (~10 μm spot diameter). The combination of strongly focused tunable X-rays with a strongly focused ultrafast laser enables both the study of atomic and molecular response to strong-optical fields and an exploration of laser-induced modification of standard X-ray processes. In addition, gas phase studies are special in that X-ray interactions with isolated atoms and molecules are amenable to first-principles theory and will provide a solid foundation for pump-probe experiments with XFELs, where strong-optical fields are expected.

The response of atoms and molecules to strong-electromagnetic fields is of significant intrinsic interest. Within the past two decades, developments in ultrafast laser technology have powered revolutionary advances in the study of light-matter interactions at high intensities (Brabec and Krausz, 2000). The diffraction-limited quality of the ultrafast laser pulses permits efficient focusing and thus with modest mJ pulse energies one can easily reach intensities of 10^{15} W/cm^2, corresponding to electric field strengths of ~10 V/Å. These external field strengths are comparable to those binding outer-shell electrons in an atom and manipulation of these electrons with strong-laser fields has led to

the discovery of many fascinating phenomena, e.g. above threshold ionization (Agostini et al., 1987), high-harmonic generation (Salières et al., 1999) and molecular alignment (Stapelfeldt and Seideman, 2003). At higher intensities in the relativistic regime ($> 10^{16}$ W/cm^2), there have been observations of laser-induced X-ray generation in clusters (McPherson et al., 1994; Ditmire et al., 1995) and even nuclear fusion (Ditmire et al., 1999).

These experiments typically use a single intense laser pulse to irradiate a gas-phase sample and analyze the products (electrons, ions, photons) to gain information on the interaction mechanisms. An independent, tunable ultrafast probe would add a valuable dimension to these studies, permitting the interrogation of state-specific atomic dynamics induced by the strong field. Earlier studies which use pump-probe techniques to study strong-field light-matter interactions have generally derived pump and probe pulses from the same laser, thus limiting both spectral tunability and pump-probe time delay range. In a pioneering experiment, Schins et al. (1994) made the first observation of laser-assisted Auger decay by using output from a single Ti:sapphire laser to provide both the "pump" IR dressing beam of $< 10^{12}$ W/cm^2 and the broadband "probe" X-rays generated from laser-irradiated liquid Ga. Subsequently, Glover et al. (1996) made the first observation of the laser-assisted photoelectric effect using an IR dressing beam combined with a family of high-harmonic probe beams within an energy range of 33–42 eV. In both cases, the Ti:sapphire lasers were multistage-amplified, and had low repetition rate and high pulse energy (10 Hz, ~40–65 mJ). In these two experiments, effect of the laser-dressing field is to cause free–free transitions in the continuum adding sidebands to the photoelectric or Auger peak in the electron energy spectrum. More recently, high harmonics have been used as probes of transient molecular alignment, (Kanai et al., 2005) again deriving the pump and probe from the same laser.

With the X-ray microprobe, there are many advantages relative to pump-probe experiments derived from a single laser. First, spectral tunability: a probe X-ray beam derived from synchrotron radiation provides wide tunability (chemical and elemental sensitivity) and independent polarization control. Second, temporal tunability: independent control of the pump laser beam and the probe X-ray beam allows delay ranges from picoseconds to milliseconds. This enables the probing of properties of individual atoms and molecules at $t = 0$ and probing of collective dynamics of the gas-phase ensemble, e.g. Coulomb explosion, at later times. Third, microfocus advantages: the micron-sized X-ray beam allows both easy target replenishment with a flowing gas or liquid source to avoid sample damage, and, efficient use of laser pulse energy. For X-ray pulses of spot diameter d separated by time Δt a flow speed of only

$d/\Delta t$ is needed to create a new target for each X-ray pulse; in our typical case $d = 10\,\mu m$, $\Delta t = 150\,ns$, the required flow velocity is only $\sim 60\,m/s$. Finally, the efficient use of laser pulse energy gives access to high-field strengths with commercial high repetition-rate lasers. Indeed, it is possible to envision X-ray probing of laser-controlled reactions using currently available frequency conversion systems having pulse energies of $\sim 50\,\mu J$ throughout the IR to UV because only modest laser intensities $\sim 10^9\,W/cm^2$ may be required.

In the following, we describe the time-resolved X-ray microprobe, give some illustrative examples from our research and provide an outlook for the future development of atomic and molecular physics with time-resolved X-ray techniques.

2. The time-resolved X-ray microprobe

Fig. 1 shows a schematic of the time-resolved X-ray microprobe at the Advanced Photon Source, Sector 7. X-rays from an undulator are routed through a Si(1 1 1) double-crystal monochromator to give a bandwidth of $\Delta E/E \sim 1.4 \times 10^{-4}$ and a flux of ~ 1 to 2×10^{13} photons/s. The source size and divergence of the X-rays give an unfocused spot size of $\sim 700\,\mu m \times 2200\,\mu m$ $(V \times H)$ FWHM at the experiment located $\sim 58\,m$ downstream from the source. We have chosen a 200-mm Kirkpa-

trick–Baez mirror pair (Eng et al., 1998) operated at $\sim 4\,mrad$ incidence angle to focus the X-rays to $\sim 10\,\mu m$ spot size in both dimensions while retaining 40% of the monochromatic flux! This corresponds to a $\sim 10^6$ X-rays per pulse that can be overlapped with a laser pulse. (Zone plates and refractive lenses commonly used in synchrotron research are less suited to our application which requires maximal flux, $\sim$micron-sized beams and longer, flexible focal distances for convenience. Zone plates give the optimal spot size 15 nm (Chao et al., 2005), but their aperture is limited, typically $\sim$100-μm, and they must be refocused for different X-ray energies. Simple refractive lenses (Dufresne et al., 2001) typically produce spot sizes $\sim 50\,\mu m$, too large for precise probing within the laser focus.) A beam position monitor located between the monochromator and the experimental apparatus is used to stabilize the vertical position of the X-ray beam to $\pm 1\,\mu m$ during a scan of the X-ray energy. Ion chambers and slits are placed at strategic locations to monitor and clean the X-ray beam.

The Ti:sapphire ultrafast laser system used to provide the strong-optical field is shown in the lower part of Fig. 1. The oscillator runs at 88 MHz and is actively synchronized to the RF of the storage ring 352 MHz (Reis et al., 2001). The output of the oscillator is stretched, amplified and recompressed in a commercial regenerative amplifier (Coherent Legend HE-USP) pumped by a diode-pumped, intracavity-doubled
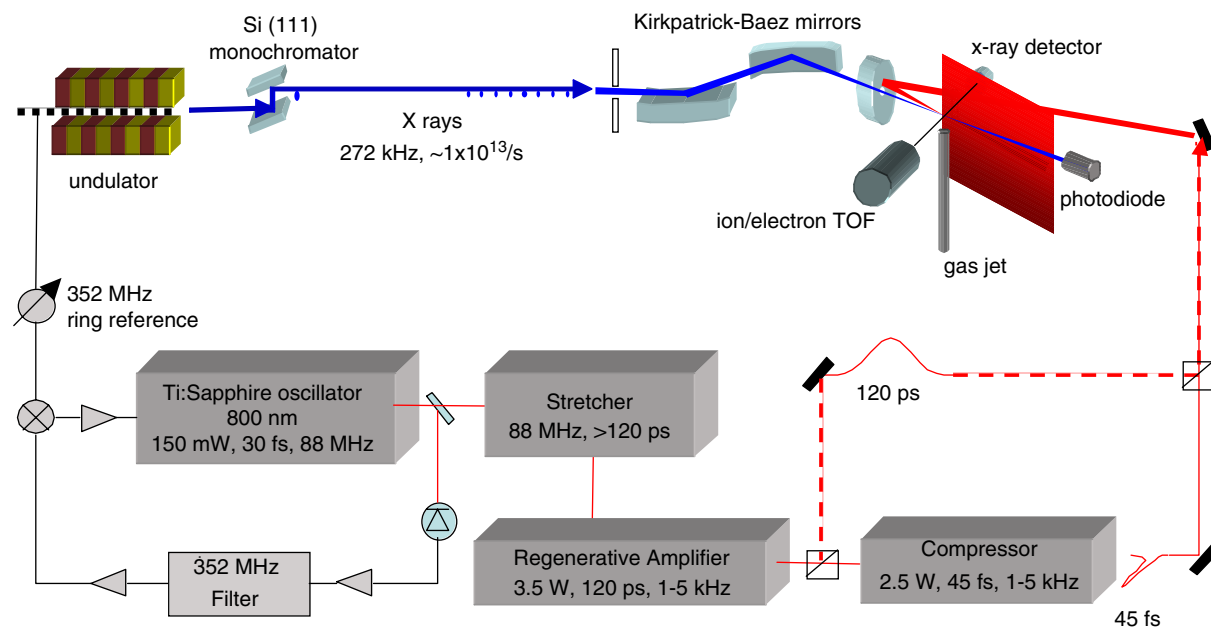

Fig. 1. Schematic of the time-resolved X-ray microprobe for atoms and molecules in the presence of strong-optical fields. Monochromatic X-rays are focused with a Kirkpatrick–Baez mirror pair to $\sim 10\,\mu m$ spot size. The X-rays probe within the interaction volume created by strong focusing of a Ti:sapphire laser with ~ 20–$100\,\mu m$ spot diameter. The interaction region is viewed by X-ray, ion and electron detectors. The target is an effusive gas jet at room temperature, with corresponding mean velocity of $\sim 300\,m/s$ for krypton.

Nd:YLF laser (Coherent Evolution-30). The compressed, amplified output has a central wavelength of ~800 nm, 2.5 W average power, pulse length ~45 fs, and a repetition rate that is variable from 1–5 kHz. The amplified output can also be diverted prior to the compressor to give chirped pulses of ~120 ps duration and ~3.5 W average power. The polarization of the laser beam can be either circular or linear with variable angle relative to the horizontally polarized X-rays by insertion of waveplates. The laser enters the rear of the vacuum chamber and is focused into the interaction region with an in-vacuum spherical mirror, $f = 100$ mm. Focusing at $f/100$ to $f/10$ is possible by varying the diameter of the input beam. A typical operating spotsize is ~100 μm FWHM.

Overlapping the two focused beams, laser and X-ray, spatially and temporally within the gas jet inside a vacuum chamber is a demanding aspect of the experiment. The focused X-rays enter the chamber through a hole in the center of the laser-focusing mirror and the two beams co-propagate through the interaction region. Rough spatial alignment at the interaction region is achieved with an in situ YAG scintillator screen observed with a lens system plus CCD camera (not shown in the figure). Fine alignment is achieved by scanning a 10-μm cross-hair through the focal volume to map the laser and X-ray foci in x, y and z. The X-ray profile is monitored either by induced current from the cross-hair or by transmission in a downstream ion chamber. The laser profile is simultaneously monitored by scatter into the lens/CCD camera setup. This method yields profile centroids to ~2 μm precision.

Temporal overlap is also a multistep process. Rough overlap at the ~0.5 ns level is done with a photodiode downstream of the interaction region. The wings of the strongly divergent laser beam are sufficient to create a sizable response in the downstream photodiode that can be observed simultaneously with the X-ray beam. Refinement of the timing is done with cross-correlation measurements using Kr ionization as explained below. The jitter between the X-rays and the amplified laser output was measured on a shot-to-shot basis using the downstream and a laser-fiducial photodiode, constant fraction discriminators and a time-to-amplitude converter to be ~3 ps.

A room temperature effusive gas jet forms the target at the interaction region. For atomic Kr, the mean velocity is $(1.33\sqrt{2kT/m})$ ~300 m/s. This is sufficient to produce a new target for the arrival of each X-ray pulse. The width of the effusive jet at the interaction region was measured to be ~2 mm FWHM. For photon-in/photon-out spectroscopy, the interaction region is viewed by X-ray detectors (silicon drift detectors) that are capable of very high count rate and good energy resolution. The photon viewing region is limited to the central portion of the Rayleigh range by in-vacuum slits. The energy resolution of the detectors (~100 eV) is sufficient to discriminate scattering from fluorescence. Alternatively, the products of the laser/X-ray interaction can be viewed by ion/electron time-of-flight detectors or an energy-resolving cylindrical mirror analyzer (CMA). For the CMA, the viewing region is limited by internal apertures. For time-of-flight spectroscopy, the position-sensitive detectors can be used to determine the location from which the ion originated.

The time structure of the Advanced Photon Source is an important consideration for laser pump/X-ray probe experiments because the two repetition rates are highly mismatched. The ring circulation period is 3.56 μs (272 kHz) The ring is run in top-off mode such that the average current is stabilized at ~100 mA. The standard fill pattern has 24 equally spaced pulses, each containing ~4 mA, separated by ~153 ns. Significantly more current can be synchronized with the 1–5 kHz laser in the "hybrid-singlet" mode, where a superbunch containing up to 16 mA is isolated by symmetrical 1.59 μs gaps from eight septets which distribute the remaining 84 mA. In addition, the long quiet period after the superbunch eases time-of-flight measurements and detector recovery. In the standard mode, only ~1/6800 of the X-ray flux can be overlapped with a 1 kHz laser, compared to 1/1700 in hybrid mode. Depending on the bunch current in the ring, the X-ray pulselength varies (Chae et al., 2001). The X-ray pulse duration in the standard (hybrid) mode is ~94 (153) ps FWHM.

3. Examples: atoms and molecules in strong optical fields

3.1. Kr ionization—cross-correlation signature and ion spectroscopy

For 800 nm light, an intensity of ~2×10^{14} W/cm^2 is sufficient to saturate ionization of Kr (Maeda et al., 2000). This intensity is easily achievable with the existing laser system. If one saturates the ionization within the laser focal volume, then the X-rays will probe an ensemble of ions, thus enabling ion spectroscopy. There is a dramatic difference between the K-edge X-ray absorption spectrum of neutral and singly ionized Kr as shown in Fig. 2.

The large pre-edge feature in singly ionized krypton corresponds to the $1s \rightarrow 4p$ resonance. Since this resonance appears only after laser-induced ionization and occurs in a region of "zero" absorption for the neutral, it is a very *clean* signature of laser/X-ray overlap. The theoretical ratio of the laser on/laser off signal when the X-rays are tuned to the $1s \rightarrow 4p$ resonance at 14.313 keV is ~40. By detecting only the Kα fluorescence channel, we isolate the K-shell absorption allowing us to observe the large laser on/laser off ratio. This ratio would be drastically decreased in a
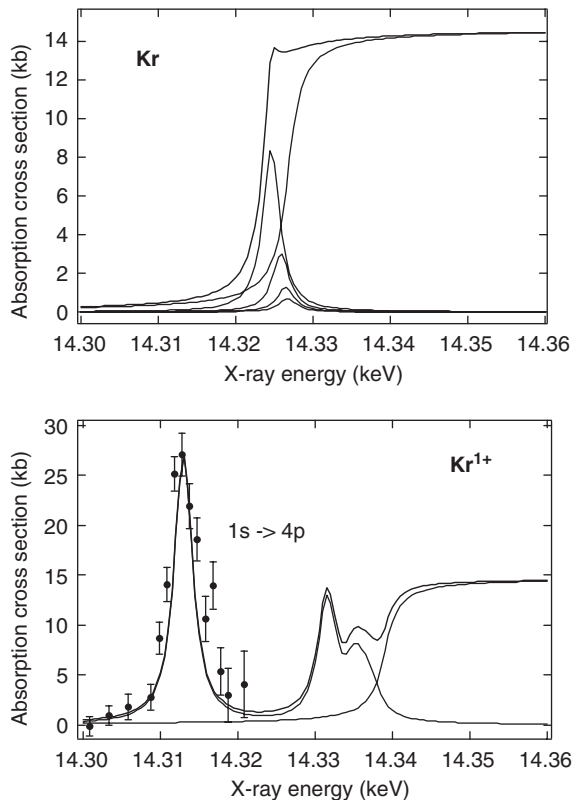
Fig. 2. Top panel: laser off: calculated K-edge absorption spectrum of neutral Kr. Lower panel: laser on: calculated K-edge absorption spectrum of singly ionized Kr. Dashed lines show discrete resonances and continuum absorption. Solid lines show the sum. Preliminary data (solid circles) show the strong resonance and are scaled to fit the calculated cross-sections.

transmission measurement. The observed laser-on/laser-off ratio approachs the theoretical value and is used to optimize spatial/temporal overlap in situ during an experiment.

Ion spectroscopy can be realized with the X-ray microprobe. The photon-in/photon-out technique permits the observation of isolated atom properties even at relatively high density. The localized gas density (1–2 mm) from the nozzle can approach $\sim 10^{14}$/cm^3. Under saturation conditions, the ion density is also $\sim 10^{14}$/cm^3 over the extent of the gas jet ~ 2 mm. (For a 100 μm beam FWHM, the beamwaist $(w_0) = 60$ μm, and the Rayleigh range of the laser focus $Z_r = \pi w_0^2 / \lambda$ exceeds the extent of the gas jet.) With this ion sample, the target thickness is $\sim 10^{13}$/cm^2, far exceeding the target thickness in a collinear ion beam setup, where the ion density is typically limited by space charge to $\sim 10^7$/cm^3 and the interaction length to ~ 100 cm.

The drawback in this scheme for ion spectroscopy is the difficulty in selectively producing a single charge state with intense pulsed lasers. As one can see from the preliminary data of the resonance region (shown in Fig. 2), the width of the resonance is greater than the theoretical lineshape, suggesting the presence of higher charge states. Indeed more extensive spectroscopic measurements combined with ion charge state measurements have confirmed the presence of Kr^{2+}. The higher charge state is formed in the central region of the laser focus. At these ion densities, the sample undergoes Coulomb expansion, which segregates the charge states in time and space. Thus, with careful spatial and temporal placement of the X-ray microprobe, the problems associated with multiple charge state production can be overcome.

3.2. Coulomb expansion of transient laser-produced plasmas

The high ion density ($\sim 10^{14}$/cm^3) produced by laser ionization is accompanied by the production of electrons; this collection of ions and electrons form a transient independent particle plasma until the electrons leave the ion vicinity determined by the laser focus (~ 100 μm). After the electrons leave, the ion assembly undergoes pure Coulomb expansion. In tunnel ionization, electrons are produced with a time-averaged kinetic energy of $U_p = 0.94 \times 10^{-13} \lambda^2$ where I (W/cm^2) is the laser intensity and λ (μm) is the laser wavelength and U_p is given in eV. For an intensity of 4×10^{14} W/cm^2 with 800 nm radiation, this corresponds to a $U_p \sim 24$ eV ($v_e \sim 3$ mm/ns). Neglecting electron recapture by the ion cloud, the electrons will leave the ion vicinity within a fraction of a nanosecond. However, electron recapture may not always be negligible with the presence of strong Coulomb attraction from the ionized core. Electron energy distributions can be controlled by varying the polarization of the strong-field ionization laser (Corkum et al., 1989) and the ensuing dynamics of the ion/electron cloud can be simulated and followed with the X-ray microprobe. Obvious extensions of the X-ray microprobe technique include the probing of dense laser-produced plasmas and laser-ablation mechanisms with spectroscopic, polarization, spatial and temporal selectivity.

3.3. Dressed atoms and molecules: molecular alignment

There are many applications for aligned molecules, ranging from studies of photoionization of fixed-in-space molecules, enhanced high-harmonic generation, optimized chemical reactivity and simplified serial single molecule crystallography with next-generation sources. Alignment can be achieved with pulsed lasers, either adiabatically or impulsively. Adiabatic laser alignment (Friedrich and Hershbach, 1995) is simply an extension of static DC field alignment, where the molecule is aligned preferentially along the laser polarization axis

due to interaction with its aniostropic polarizability. Two requirements for the adiabatic aligning laser pulses exist. The field strength that can be imposed is limited by the threshold for ionization, e.g. $\sim 10^{12}\,\text{W/cm}^2$ for I_2. The laser pulse length must be significantly longer than the molecular rotational period, $\tau_{\text{laser}>}\tau_{\text{rot}}$, for the alignment to evolve adiabatically. In the presence of the aligning field, the free rotor evolves into an eigenstate of the complete Hamiltonian, i.e. a "pendular" state. As the laser field decays, the alignment is lost, as illustrated in Fig. 3a.

In contrast, with the impulsive scheme, molecules are aligned *subsequent* to passage of a short laser pulse. The impulse coherently excites a superposition of rotational states to create an aligned ensemble that then decays and revives at predictable intervals (Seideman, 1999; Ortigoso et al., 1999), as illustrated in Fig. 3b. A full revival is observed to occur after a rotational period $T = 1/2Bc$ where B is the rotational constant of the molecule in cm^{-1} and c is the speed of light. Partial revivals occur at $T/4$, $T/2$, $3T/4$ (Rosca-Pruna and Vrakking, 2001). The revival duration is dependent upon the interplay between molecular and laser pulse parameters but typically lasts for no more than a few picoseconds. The advantage for many applications is that molecules are aligned under field-free conditions.

In order to study inner-shell photoionization from aligned molecules, one can use the X-ray microprobe to interrogate the aligned molecule. With the current pulse length at the Advanced Photon Source, ~ 100 ps, it would be impossible to interrogate the impulsively aligned molecules. However, to probe adiabatically aligned molecules, the alignment laser pulse must simply be longer than the X-ray pulse. This is possible with the current laser system by diverting the amplified output prior to recompression to achieve ~ 120 ps pulses, as shown in Fig. 1 by the dashed line. Typically, adiabatic alignment is done with low repetition rate, 10 ns pulse length lasers. However, with microfocus conditions, adiabatic alignment at kHz repetition rates is feasible thus enabling studies of synchrotron-based X-ray photoionization from dressed atoms and molecules (i.e. aligned) with reasonable count rates.

4. Future outlook—1-ps X-rays at the Advanced Photon Source

While most of the applications discussed above can be realized with the presently available bunch lengths from the Advanced Photon Source ~ 100-ps FWHM, they would clearly benefit from shorter pulses of ~ 1-ps duration. In addition to the 100-fold increase in time-resolution, one also obtains a similar increase in accessible field strength for dressed-state and coherent control studies in atoms and molecules (Rice and Zhao, 2000).

An ingenious scheme to produce subpicosecond X-ray pulses in a storage ring was proposed by Zholents et al. (1999). The basic concept is that a transversely deflecting RF cavity in the storage ring structure can be used to create a vertical or angular displacement that is correlated with the longitudinal position within an electron bunch. A second cavity placed at a vertical phase advance $n\pi$ downstream of the first cancels the correlation. The transverse displacement can be made large enough such that the X-ray radiation from the bunch can be considered as a large number of independent sources, each of which would have a duration of ~ 1 ps. Ideally, only the section of the storage ring between the two cavities would have short pulses; the impact on the rest of the ring would be negligible. This concept has been intensively investigated over the past year at the Advanced Photon Source both in simulation by Borland (2005) and in practice by Guo et al. (2005). The simulations show that the concept is practical and the test beam studies confirm the accuracy of the simulation parameters. The source parameters are currently being refined, and recently it has been discovered that an early concern, vertical emittance growth throughout the ring (Borland, 2005), can be largely eliminated, even at the high deflection voltage needed for the shortest pulses (Borland and Sajaev, 2005).
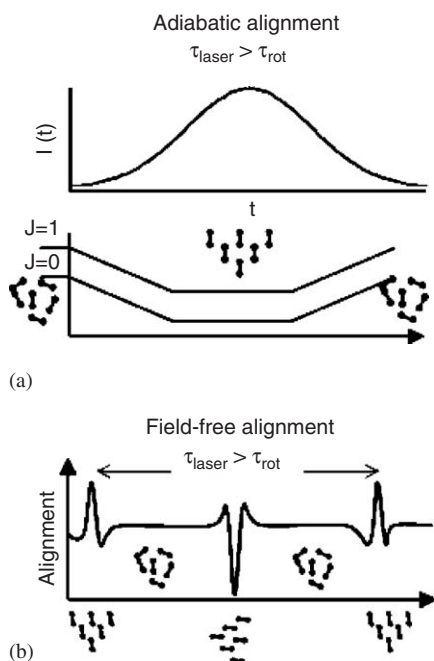
Fig. 3. (a) Schematic of adiabatic alignment. Molecules are aligned during the presence of strong laser field. (b) Schematic of field-free alignment. Molecules are aligned at predictable intervals after an impulsive laser pulse.

The availability of a high-repetition rate, short-pulse X-ray source will vastly increase the current parameter space available for time-resolved X-ray studies. Table 1 lists working parameters for the APS storage ring and the specifications for the LCLS XFEL. The parameters for the simulated 1-ps storage-ring source are shown in parentheses in the second column. For the LCLS, parameters for two modes are shown, the 8000 and the 800 eV modes in parentheses. Although the expected pulse duration is ∼5-fold longer than initial specifications at LCLS, the average power is similar and there are a number of advantages of the storage ring RF deflection method namely: a high-repetition rate 6.5 MHz compared to 120 Hz; modest fluence 10^8 X-rays per pulse (for reduced sample damage and suitability for time-resolved probes) compared to high fluence 10^{12} X-rays per pulse; well-characterized temporal and energy profiles compared to chaotic profiles with large shot-to-shot variation; simultaneous users at multiple wavelengths compared to single users; existing detector and signal processing techniques compared to required development of single-shot techniques and advanced detectors.

A practical issue is the relatively large vertical beamsize of the chirped X-ray pulse. The angular deflection correlates with time at a slope of ∼380 μrad/40 ps RMS pulse in the APS storage ring. Thus, at the location of the X-ray optics, 30 m downstream, a vertical beamsize of ∼11 mm for the chirped X-ray pulse is formed. A simple sub-mm slit at this position could yield a pulse length of a few ps FWHM. This slitted beam could be used for spectroscopy in energy-dispersive mode (Pettifer et al., 2005) to accumulate an X-ray spectrum over the entire unduator bandwidth in transmission mode with ∼1 ps resolution. In addition, many condensed matter diffraction experiments are not photon limited, and the simple slit would greatly improve the time resolution achievable. It is also possible to use asymmetrically cut crystals and mirrors

to compress the X-ray pulse in both time and space and increase the flux ∼10-fold over that achieved by simple slitting at the same pulse duration (Shastri, 2005). Thus, it is reasonably straightforward to advance to the 1-ps timescale using a storage-ring-based source coupled with existing technology.

As a complement to the chirped-pulse storage ring concept, XFELs produce the shortest pulse duration and highest intensity in the hard X-ray region. Indeed, XFEL enhancement schemes based upon emittance spoiling (Emma et al., 2004) and further phase space manipulation of the electron beam (Zholents and Fawley, 2004) suggest that pulses of few femtosecond and even attosecond duration are possible! Initial experiments with baseline parameters at the XFEL must diagnose XFEL output which will have pulse-to-pulse fluctuations in temporal (and hence spectral) profiles since the SASE lasing process is initiated from noise. Atomic and molecular physics is expected to play a key role here as the simplicity of the target permits close coupling of ab initio theory with experiment to understand strong-field interactions at short wavelengths.

5. Summary

X-ray microprobe techniques can be particularly advantageous for time-resolved studies via pump-probe techniques. In particular, microfocused X-rays can probe focal volumes where laser intensities of up to ∼10^{15} W/cm^2 can be present using a commercial regeneratively amplified Ti:sapphire laser system. The full power of tunable-synchrotron radiation then allows the detailed probing of strong-field-induced processes, e.g. the Coulomb expansion dynamics of an independent particle plasma produced by tunnel ionization in a gas and the tunnel ionization process itself. The efficient utilization of available laser power via microfocusing permits the study of molecular alignment at kHz

Table 1
Comparison of APS vs. LCLS X-ray sources

Parameter	APS storage ring	LCLS XFEL
Pulse duration FWHM	∼100 ps (1.5 ps)	<230 fs
Repetition rate	6.5 MHz	120 Hz
Photons/pulse	∼10^8	∼1.1×10^{12} (∼2.8×10^{13})
Photon energy	∼3-35 keV	∼8.2(0.82) keV
Energy bandwidth	∼10^{-2}	0.06(0.24)%
Beam size $\sigma_x \times \sigma_y$	254×12 μm (245×12 μm)	28 μm σ_{rms} (31 μm)
Beam divergence $\sigma'_x \times \sigma'_y$	15.6×3.0 μrad (12.3×2.2 μrad)	0.43 μrad σ_{rms} (3.8 μrad)
Temporal profile	Gaussian	Chaotic
Spectral profile	Smooth	Chaotic

APS photon beam parameters are given for Undulator A (Dejus et al., 2002). LCLS photon beam parameters from LCLS Conceptual Design report (Arthur et al., 2002).

repetition rates, making such experiments feasible in a storage ring environment. Finally, the generation of ~1-ps X-ray pulses at the Advanced Photon Source appears to be practical, enhancing both the temporal resolution and attainable dressing-intensity 100-fold and enabling exciting new science.

Acknowledgments

References

Agostini, P., Fabre, F., Mainfray, G., Petite, G., Rahman, N.K., 1987. Free-free transitions following six-photon ionization of xenon atoms. Phys. Rev. Lett. 42, 1127.

Arthur, J., et al., 2002. Linac Coherent Light Source (LCLS) Conceptual Design Report, SLAC-R-593.

Bargheer, M., Zhavoronkov, N., Gritsai, Y., Woo, J.C., Kim, D.S., Woerner, M., Elsaesser, T., 2004. Coherent atomic motions in a nanostructure studied by femtosecond x-ray diffraction. Science 306, 1771–1773.

Borland, M., 2005. Simulation and analysis of using deflecting cavities to produced short X-ray pulses with the Advanced Photon Source. Phys. Rev. ST Accel. Beams 8, (074001-1–074001-18).

Borland, M., Sajaev, V., 2005. Simulations of X-ray slicing and compression using crab cavities in the Advanced Photon Source. In: Proceedings of the Particle Accelerator Conference, PAC 2005, pp. 3886–3888.

Brabec, T., Krausz, F., 2000. Intense few-cycle laser fields. Rev. Mod. Phys. 72, 545–591.

Cavalleri, A., Rini, M., Chong, H.H.W., Fourmaux, S., Glover, T.E., Heimann, P.A., Kieffer, J.C., Schoenlein, R.W., 2005. Band-selective measurements of electron dynamics in VO_2 using femtosecond near-edge X-ray absorption. Phys. Rev. Lett. 95, 067405-1–067405-4.

Chae, Y.-C., Emery, L., Lumpkin, A.H., Song, J., Yang, B.X., 2001. Measurement of the longitudinal microwave instability in the APS storage ring. In: Proceedings of the Particle AcceleratorConference, Chicago, Illinois, 2001. IEEE, Piscataway, NJ, pp. 1817–1819.

Chao, W., Harteneck, B.D., Liddle, J.A., Anderson, E.H., Attwood, D.T., 2005. Soft X-ray microscopy at a spatial resolution better than 15 nm. Nature 435, 1210–1213.

Chen, L.X., Jäjer, W.J.H., Jennings, G., Gosztola, D.J., Munkholm, A., Hessler, J.P., 2001. Capturing a photo-excited molecular structure through time-domain X-ray absorption fine structure. Science 292, 262–264.

Corkum, P.B., Burnett, N.H., Brunel, F., 1989. Above-threshold ionization in the long-wavelength limit. Phys. Rev. Lett. 62, 1259–1262.

Davidsson, J., Poulsen, J., Cammarata, M., Georgiou, P., Wouts, R., Katona, G., Jacobson, F., Plech, A., Wulff, M., Nyman, G., Neutze, R., 2005. Structural determination of a transient isomer of CH_2I_2 by picosecond X-ray diffraction. Phys. Rev. Lett. 94, 245503-1–245503-4.

DeCamp, M.F., Reis, D.R., Cavalieri, A., Bucksbaum, P.H., Clarke, R., Merlin, R., Dufresne, E.M., Arms, D.A., Lindenberg, A.M., MacPhee, A.G., Chang, Z., Lings, B., Wark, J.S., Fahy, S., 2003. Transient strain driven by a dense electron-hole plasma. Phys. Rev. Lett. 91, 165502-1–165502-4.

Dejus, R., Vasserman, I.B., Sasaki, S., Moog, E.R., 2002. Undulator a magnetic properties and spectral performance. ANL/APS/Tech. Bull. 45, 1–51.

Ditmire, T., Donnelly, T., Falcone, R.W., Perry, M.D., 1995. Strong X-ray emission from high-temperature plasmas produced by intense irradiation of clusters. Phys. Rev. Lett. 75, 3122–3125.

Ditmire, T., Zweiback, J., Yanovsky, V.P., Cowan, T.E., Hays, G., Wharton, K.B., 1999. Nuclear fusion from explosions of femtosecond laser-heated deuterium clusters. Nature 398, 489–492.

Dufresne, E.M., Arms, D.A., Clarke, R., Pereira, N.R., Dierker, S.B., Foster, D., 2001. Lithium metal for X-ray refractive optics. Appl. Phys. Lett. 79, 4085–4087.

Emma, P., Bane, K., Cornacchia, M., Huang, Z., Schlarb, H., Stupakov, G., Walz, D., 2004. Femtosecond and subfemtosecond x-ray pulses from a self-amplified spontaneous-emission-based free-electron laser. Phys. Rev. Lett. 92, 074801-1–074801-4.

Eng, P.J., Newville, M., Rivers, M.L., Sutton, S.R., 1998. Dynamically figured Kirkpatrick Baez X-ray micro-focusing optics. SPIE Proc. 3449, 145–156.

Friedrich, B., Hershbach, D., 1995. Alignment and trapping of molecules in intense laser fields. Phys. Rev. Lett. 74, 4623–4626.

Glover, T.E., Schoenlein, R.W., Chin, A.H., Shank, C.V., 1996. Observation of laser assisted photoelectric effect and femtosecond high order harmonic radiation. Phys. Rev. Lett. 76, 2468–2471.

Guo, W., Borland, M., Harkay, K., Sajaev, V., Yang, B., 2005. Generating picosecond X-ray pulses with beam manipulation in synchrotron light sources. In: Proceedings of the Particle Accelerator Conference, PAC 2005, pp. 3898–3900.

Ihee, H., Lorenc, M., Kim, T.K., Kong, Q.Y., Cammarata, M., Lee, J.H., Bratos, S., Wulff, M., 2005. Ultrafast X-ray diffraction of transient molecular structures in solution. Science 309, 1223–1227.

Kanai, T., Minemoto, S., Sakai, H., 2005. Quantum interference during high-order harmonic generation from aligned molcules. Nature 435, 470–474.

King, W.E., Campbell, G.H., Frank, A., Reed, B., Schmerge, J.F., Siwick, B.J., Stuart, B.C., Weber, P., 2005. Ultrafast electron microscopy in materials science, chemistry and biology. J. Appl. Phys. 97, 111101.

Lindenberg, A.M., Kang, I., Johnson, S.L., Missalla, T., Heimann, P.A., Chang, Z., Larsson, J., Bucksbaum, P.H., Kapteyn, H.C., Padmore, H.A., Lee, R.W., Wark, J.S.,

Falcone, R.W., 2000. Time-resolved X-ray diffraction from coherent phonons during a laser-induced phase transition. Phys. Rev. Lett. 84, 111–114.

Lindenberg, A., et al., 2005. Atomic scale visualization of inertial dynamics. Science 308, 392–395.

Maeda, H., Dammasch, M., Eichmann, U., Sandner, W., Becker, A., Faisal, F.H.M., 2000. Strong-field multiple ionization of krypton. Phys. Rev. A 62, 035402-1–035402-4.

McPherson, A., Thompson, B.D., Borisov, A.B., Boyer, K., Rhodes, C.K., 1994. Nature 370, 631–634.

Neutze, R., Wouts, R., Techert, S., Davidson, J., Kocsis, M., Kirrander, A., Schotte, F., Wulff, M., 2001. Visualizing photochemical dynamics in solution through picosecond X-ray scattering. Phys. Rev. Lett. 87, 195508-1–195508-4.

Ortigoso, J., Rodríguez, M., Gupta, M., Friedrich, B., 1999. Time evolution of pendular states created by the interaction of molecular polarizability with a pulsed nonresonant laser field. J. Chem. Phys. 110, 3870–3875.

Pettifer, R.F., Mathon, O., Pascarelli, S., Cooke, M.D., Gibbs, M.R.J., 2005. Measurement of femtometre-scale atomic displacements by X-ray absorption spectroscopy. Nature 435, 78–81.

Plech, A., Wulff, M., Bratos, S., Mirloup, F., Vuilleumier, R., Schotte, F., Anfinrud, P.A., 2004. Visualizing chemical reactions in solution by picosecond X-ray diffraction. Phys. Rev. Lett. 92, 125505-1–125505-4.

Reis, D.A., DeCamp, M.F., Bucksbaum, P.H., Clarke, R., Dufresne, E., Hertlein, M., Merlin, R., Falcone, R., Kapteyn, H., Murnane, M.M., Larsson, J., Missalla, Th., Wark, J.S., 2001. Probing impulsive strain propagation with X-ray pulses. Phys. Rev. Lett. 86, 3072–3075.

Rice, S.A., Zhao, M., 2000. Optical Control of Molecular Dynamics. Wiley, New York.

Rosca-Pruna, F., Vrakking, M.J.J., 2001. Experimental observation of revival structures in picosecond laser-induced alignment of I_2. Phys. Rev. Lett. 87, 153902-1–153902-4.

Saes, M., Bressler, C., Abela, R., Grollimund, D., Johnson, S.L., Heimann, P.A., Chergui, M., 2003. Observing photochemical transients by ultrafast X-ray absorption spectroscopy. Phys. Rev. Lett. 90, 047403-1–047403-4.

Salières, P., L'Huillier, A., Antoine, P., Lewenstein, M., 1999. Study of the spatial and temporal coherence of high-order harmonics. Adv. Atom. Mol. Phys. 41, 83–142.

Schins, J.M., Breger, P., Agostini, P., Constantinescu, R.C., Muller, H.G., Grillon, G., Antonetti, A., Mysyrowicz, A., 1994. Observation of laser-assisted Auger decay in argon. Phys. Rev. Lett. 73, 2180–2183.

Schoenlein, R.W., Chattopadhyay, S., Chong, H.H.W., Glover, T.E., Heimann, P.A., Shank, C.V., Zholents, A.A., Zolotorev, M.S., 2000. Generation of femtosecond pulses of synchrotron radiation. Science 287, 2237–2240.

Seideman, T., 1999. Revival structure of aligned rotational wave packets. Phys. Rev. Lett. 83, 4971–4974.

Shastri, S., 2005. Private communication.

Siwick, B., Dwyer, J.R., Jordan, R.E., Miller, R.J.D., 2003. An atomic-level view of melting using femtosecond electron diffraction. Science 302, 1382–1385.

Sondhauss, P., Larsson, J., Harbst, M., Naylor, G.A., Plech, A., Scheidt, K., Synnergren, O., Wulff, M., Wark, J.S., 2005. Picosecond X-ray studies of coherent folded acoustic phonons in a multiple quantum well. Phys. Rev. Lett. 94, 125509-1–1125509-4.

Stapelfeldt, H., Seideman, T., 2003. Aligning molecules with strong laser pulses. Rev. Mod. Phys. 75, 543–557.

Stöhr, J., 1996. NEXAFS Spectroscopy. Springer, Berlin.

Tschentscher, Th., 2004. Investigation of ultrafast processes using X-ray free-electron laser radiation. Chem. Phys. 299, 271–276.

Zewail, A., 2003. Nobel lectures. In: Grenthe, I. (Ed.), Chemistry 1996–2000. World Scientific, Singapore, pp. 274–367.

Zewail, A., 2005. Diffraction, crystallography and microscopy beyond three diminsions, strucural dyamics in space and time. Phil. Trans. R. Soc. A 364, 315–329.

Zholents, A.A., Fawley, W.M., 2004. Proposal for intense attosecond radiation from an X-ray free-electron laser. Phys. Rev. Lett. 92, 224801-1–224801-4.

Zholents, A., Heimann, P., Zolotorev, M., Byrd, J., 1999. Generation of subpicosecond X-ray pulses using RF orbit deflection. Nucl. Instrum. Methods Phys. Res. Sect. A 425, 385–389.